Coexistence pressure for a martensitic transformation from theory and experiment: Revisiting the bcc-hcp transition of iron under pressure

N. A. Zarkevich and D. D. Johnson

Phys. Rev. B **91**, 174104 — Published 12 May 2015

DOI: 10.1103/PhysRevB.91.174104

Coexistence pressure for a martensitic transformation from theory and experiment: revisiting the bcc-hcp transition of iron under pressure

N. A. Zarkevich,[1] and D. D. Johnson[1,2*]
[1] *The Ames Laboratory, U.S. Department of Energy, Ames, Iowa 50011-3020 USA; and*
[2] *Materials Science & Engineering, Iowa State University, Ames, Iowa 50011-2300 USA.*

The coexistence pressure of two phases is a well-defined point at fixed temperature. In experiment, however, due to non-hydrostatic stresses and a stress-dependent potential energy barrier, different measurements yield different ranges of pressure with a hysteresis. Accounting for these effects, we propose an inequality for comparison of the theoretical value to a plurality of measured intervals. We revisit decades of pressure experiments on the *bcc* ↔ *hcp* transformations in iron, which are sensitive to non-hydrostatic conditions and sample size. From electronic-structure calculations, we find a *bcc* ↔ *hcp* coexistence pressure of 8.4 GPa. We construct the equation of state for competing phases under hydrostatic pressure, compare to experiments and other calculations, and address the observed pressure hysteresis and range of onset pressures of the nucleating phase.

PACS numbers: 64.70.K-, 05.70.Fh, 02.70.-c, 81.05.Bx

I. INTRODUCTION

Knowledge of the equation of state is crucially important in materials science and engineering, metallurgy, geophysics, and planetary sciences. However, equilibrium coexistence of phases during a pressure-induced martensitic transformation is extremely difficult to realize experimentally, and most shock and anvil cell experiments contain various amounts of a non-hydrostatic, anisotropic stress. Hence, an improved understanding of transformations arises when we can better compare idealized theoretical results to realistic experimental data. A long-studied case is iron (Fe), our focus below, but the results remain quite general.

Iron is the most stable element produced by nuclear reactions at ambient pressure, and one of the most abundant elements in the Earth. Thus, magneto-structural transformations[1–28] and high-pressure states[29–69] in iron attract enormous interest, especially in geophysics because iron is a primary constituent of the Earth's core,[29–163] many meteorites,[163–172] and, due to its properties and availability, most steels.[173] At low pressure P and temperature T, the α-phase of iron is a ferromagnet (FM) with the body-centered cubic (bcc) structure. At higher pressures, iron transforms to the ε-phase with hexagonal close-packed (hcp) structure of higher density that is non-magnetic or weakly anti-ferromagnetic. This transformation is martensitic,[3] and the bcc-hcp equilibrium coexistence pressure is difficult to determine unambiguously experimentally (Table 1).

A martensitic transformation between bcc (α) and hcp (ε) phases can be characterized by four pressures (Table I): a *start* and *end* pressure of direct $\alpha \to \varepsilon$ ($P^{\alpha\to\varepsilon}_{start}$, $P^{\alpha\to\varepsilon}_{end}$) and reverse $\varepsilon \to \alpha$ ($P^{\varepsilon\to\alpha}_{start}$, $P^{\varepsilon\to\alpha}_{end}$) transformations. Because martensitic stress is present in the anisotropic hcp phase but not in the isotropic bcc phase, we suggest the inequality

$$P^{\varepsilon\to\alpha}_{end} < P_0 < P^{\alpha\to\varepsilon}_{start} \qquad (1)$$

for the $\alpha - \varepsilon$ equilibrium coexistence pressure P_0 and the observed hysteresis, rather than an inaccurate simple average[3] $P^{avg.}_{start} = \frac{1}{2}\left(P^{\alpha\to\varepsilon}_{start} + P^{\varepsilon\to\alpha}_{start}\right)$.

The inequality (1) is applicable to all first-order structural transformations from an isotropic phase (e.g., Fe α-phase) with well-defined and reliably measurable P and T to one more prone to measurement error (e.g., anisotropic Fe ε-phase). This inequality is a generalization of what is expected in the classic liquid-gas isotherm in Fig. 1 from the van der Waals equation of state (EoS).[174] If P and T are reliably measured in gas (G), but not in liquid (L) phase, then the isothermal equilibrium coexistence pressure P_0 at a given T is bounded by $P^{L\to G}_{end} < P_0 < P^{G\to L}_{start}$, which is identical to (1). From the EoS,[174] the overheated liquid and overcooled gas are observed during fast adia-

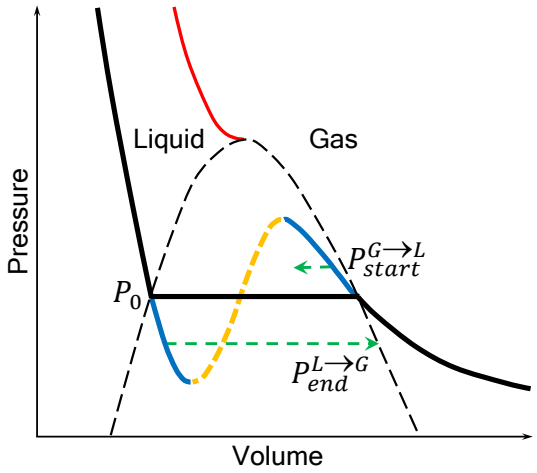

FIG. 1: van der Waals isotherm (solid black), along with the unstable region (dashed yellow), and metastable overheated liquid and overcooled gas (blue). Delayed start of condensation and end of evaporation (dashed green arrows). Liquid and gas are indistinguishable at the critical isotherm (red) above the phase segregated region (dashed black line).

batic processes or in a clean medium deprived of defects, able to serve as centers of evaporation and condensation. Due to heat of evaporation and condensation, and a limited thermal conductivity, it takes a very long time to maintain a constant temperature in both phases. In a faster process, start of condensation is delayed, and evaporation produces a cooled gas; hence, $P_{end}^{L\to G}$ is on a lower isotherm, as in Fig. 1. Inequality (1) is applicable both to solid-solid and liquid-gas transformations, which have a hysteresis due to nucleation barriers.

For iron, while shock and anvil-cell (AC) pressure experiments give different averages $P_{start}^{avg.}$, they satisfy the more appropriate inequality (1), see Table I and Fig. 2d. To make direct and quantitative connections, we calculate the hydrostatic EoS of α and ε Fe, determine P_0 via common-tangent construction, which should be thermodynamically relevant to purely hydrostatic equilibrium, and compare the result to experiment.

II. BACKGROUND

Previous Experiments: Shock and AC pressure experiments are the major approaches to measure pressure-induced transformations, although hydrostatic conditions are often difficult to assess. Experimental onset (start) and final (end) pressures for $\alpha \to \varepsilon$ and $\varepsilon \to \alpha$ transformations are summarized in Table 1, which show a large span and the reason to revisit this issue.

For completeness, we highlight the experiments and their outcome for iron. Bancroft *et al.*[1] studied propagation of compressive waves generated by high explosive in Armco iron and reported a polymorphic transition at 13.1 GPa. Balchan and Drickamer[2] used a high-pressure electrical resistance cell and found a sharp rise in resistance of iron at 13.3 GPa. Giles *et al.*[3] showed that this bcc-hcp transformation is martensitic; their estimate of P_0 by $P_{start}^{avg.} = 10.7 \pm 0.8\,\mathrm{GPa}$ differs from the earlier reported $P_{start}^{\alpha\to\varepsilon} = 13\,\mathrm{GPa}$, often quoted as the martensitic start pressure. Mao, Bassett, and Takahashi[5] performed XRD measurements of lattice parameters of iron at 23°C at pressures up to 30 GPa, and suggested a bcc-hcp shear-shuffle model (their Fig. 3 is reproduced in Ref. 6). Bassett and Huang[6] applied a non-hydrostatic pressure with an uncontrolled shear strain (known to produce pressure self-multiplication)[175] and confirmed an atomic mechanism[5] of the bcc-hcp transition, but omitted discussion of changes in volume and magnetization in their shear-shuffle model. Zou *et al.*[4] used solid He as the pressure medium in their diamond AC (DAC) experiments on iron (99.95 wt.% Fe) powder pressed into a plate and on a folded section of a 10 micron foil; they pointed at the uniform non-hydrostatic stress as a possible cause of differing data.

Importantly, transition pressure estimates depend on how hydrostatic the applied stress is and sample size. For example, Bargen and Boehler[8] found that the pressure interval of the forward bcc→hcp transition increases with increasing non-hydrostaticity (transition pressures and hysteresis width change systematically with the shear strength of the pressure medium).[7] The best pressure medium is a superfluid; a good one is a gas or a fluid with a low viscosity; the worst one is a viscous fluid or a solid. Due to grain boundaries[176] and melting-freezing waves,[177] solid helium (He) can behave as a superfluid.[178]

Taylor *et al.*[9] focused on the large hysteresis and used a DAC up to 24 GPa; as pressure is increased, Fe is fully converted to hcp at $P_{end}^{\alpha\to\varepsilon} = 23\,\mathrm{GPa}$. Upon reducing pressure, half of the hcp transforms to bcc by $P_{1/2}^{\varepsilon\to\alpha} = 9.5\,\mathrm{GPa}$, while a small ε-Fe remnant is present at $P_{end}^{\varepsilon\to\alpha} = 7.7\,\mathrm{GPa}$. They report $P_{start}^{\alpha\to\varepsilon}$ values from 8.6 to 15 GPa[9]. Using a radial diffraction DAC with infrared laser heating on Alfa Aesar (99.9% pure) Fe powder (10^{-5} m particle size), Miyagi *et al.*[14] reported appearance of hcp at 10 GPa that fully converts near 22 GPa, while bcc appears at 8 GPa during decompression. Jiang *et al.*[12] studied grain-size and alloying effects on the transition pressure, finding that $P_{start}^{\alpha\to\varepsilon}$ shifts from 13 GPa in bulk to 11 GPa in nano-crystalline samples. Wang, Ingalls, and Crozier[10] performed an XAFS study at 23°C up to 21.5 GPa; a mixed-phase region was found between $P_{start}^{\alpha\to\varepsilon} = 13$ and $P_{end}^{\alpha\to\varepsilon} = 20\,\mathrm{GPa}$, and between $P_{start}^{\varepsilon\to\alpha} = 15$ and $P_{end}^{\varepsilon\to\alpha} = 11$ GPa. Later, Wang and Ingalls[11] used XAFS with a sintered boron-carbide anvil cell to measure lattice constants and bcc abundance versus P, and reported $P_{start}^{\alpha\to\varepsilon} = 13\,\mathrm{GPa}$ and $6.6 \le P_{end}^{\varepsilon\to\alpha} \le 8.9$ GPa. Using *in situ* EXAFS measurements and nanosecond laser shocks, Yaakobi *et al.*[15] detected hcp phase and claimed that the $\alpha \to \varepsilon$ transition can happen very quickly.

Finally, the change of magnetization along a transition path is important, where there is an abrupt 8–10% volume decrease at the transition state[6,13]. Baudelet *et al.*[13] combined x-ray absorption spectroscopy (XAS) and x-ray magnetic circular dichroism (XMCD) on a sample in a CuBe DAC and found a transition at 14 GPa, with a $2.4 \pm 0.2\,\mathrm{GPa}$ width of the local structural transition and a $2.2 \pm 0.2\,\mathrm{GPa}$ width of the magnetic one; they suggest that the magnetic moment collapse lies at the origin of the structural transition, and slightly precedes the structural one.

Previous Theory Results: Former bcc-hcp equilibrium pressure calculations provided values of 13.1 GPa,[19] 11 GPa,[207] 10.5 GPa,[24] and 10 GPa,[25] in apparent agreement with the experimental values of $P_{start}^{\alpha\to\varepsilon} = 13\,\mathrm{GPa}$[1–3] and $P_{start}^{avg.} = 10.7 \pm 0.8\,\mathrm{GPa}$.[3] However, those calculated pressures disagree with later experimental data (Table 1). Using *ab initio* molecular dynamics (MD), Belonoshko *et al.*[85,179–183] considered shear at the Earth's core conditions[86,87] and constructed an EoS for α[40,182] and ε[183] Fe. Wang *et al.*[23] studied nucleation of the higher-pressure hcp and fcc phases by classical MD simulations employing an embedded atom method (EAM) potential, and found that the transformation happens on a picosecond timescale; their calculated transition pressure is around 31-33 GPa for uniform[23] and 14 GPa for

Ref.	Year	$P^{\alpha\to\varepsilon}_{start}$	$P^{\alpha\to\varepsilon}_{end}$	$\Delta P^{\alpha\to\varepsilon}$	$P^{\varepsilon\to\alpha}_{start}$	$P^{\varepsilon\to\alpha}_{end}$	$\Delta P^{\varepsilon\to\alpha}$	Expt.
[1]	1956	13.1						shock
[2]	1961	13.3						resistance
[3]	1971	13.3	16.3	3	8.1	4.5	3.6	AC
[4]	1981	13.52	15.27	<2	9.2	6.74	2.5	powder
[4]		15.21	15.47	<1	10.23	8.5(6)	2	foil
[6]	1987	10.8	21	≈10	15.8	3	13	Au
[7]	1990	10.6	25.4	14.8	16	4	12	Al_2O_3
[7]		10.7	21.6	10.9	16.2	3.7	12.5	Au
[7]		12.4	17.8	5.4	12.2	4.8	7.4	NaCl
[7]		12.8	17.2	4.4	11.8	5.5	6.3	CsI
[7]		14.3	17.5	3.2	11.9	7	5	m-e
[7]		14.9	<15.9	0.5	<11	>7	<4	Ar
[7]		15.3	15.3	0.1	10.6	8.0(6)	2	He
[9]	1991	8.6	23	≈14	[9.5]	7.7	3.6	hydrostatic
[11]	1998	13.0	18.6	≈5.6	[10.3]	6.6	7.4	XAFS
[12]	2001	13	17	≈4	8	5	3	bulk
[12]		11	14	≈3	7	1	6	nano-Fe
[13]	2005	14	16	2.4				AC
[14]	2008	10	22	≈12	8	4	4	powder

TABLE I: Start and end pressures [GPa] with width $\Delta P = |P_{end} - P_{start}|$ for iron bcc (α) – hcp (ε) direct and inverse transformations. Type of experiment (Expt.) specifies shock or anvil cell (AC), form of sample (bulk, foil, powder), or pressure medium (He, Ar, m-e for methanol-ethanol, etc.) in the AC. The $P^{\varepsilon\to\alpha}_{1/2}$ values at half-transition (50% bcc + 50% hcp) are in the square brackets [$P^{\varepsilon\to\alpha}_{start}$ column].

uniaxial[22] compression (but there is no magnetization in the EAM potential). Caspersen *et al.*[26] showed that presence of a modest shear accounts for the scatter in measured transformation pressures, affecting the hysteresis. Johnson and Carter[19] used a drag method in a rapid-nuclear-motion (RNM) approximation and obtained an unphysical discontinuous jump in atomic shuffle degrees of freedom, giving a very low bcc-hcp barrier; they found that bcc and hcp phases have equal enthalpies at the calculated pressure of 13.1 GPa.

Liu and Johnson[20] directly constructed the potential energy surface in a 2-atom cell for the shear-shuffle model,[6] allowing changes of lattice constants and (continuous) atomic degrees of freedom; although hydrostatic pressure cannot produce shear, pressure does affect the potential energy surface and barriers. They reported ≈9 GPa for bcc-hcp coexistence; the calculated kinetic barriers along the transition path were 132 meV/atom at 0 GPa with an estimated minimum (maximum) onset pressure of 9 (12.6) GPa, 119 meV/atom at 10.5 GPa with a min (max) onset at 8.1 (13.8) GPa, and 96 meV/atom at 22 GPa with a min (max) onset of 6.6 (10.2) GPa. That is, there is an expected 3.6 to 5.7 GPa hysteresis width depending on kinetic pathway (and volume fluctuations). In addition, they showed that drag methods decouple degrees of freedom incorrectly, as confirmed later.[184]

Recently, Dupe *et al.*[186] reconsidered the transition mechanism within the same shear-shuffle model,[6] but incorrectly fixed the volume at 71.5 bohr^3/atom (no volume collapse allowed), and used the RNM drag method to compare energies of three shuffling mechanisms at constant shear and volume. Friak and Sob[24] in a 4-atom cell considered non-magnetic (NM) and antiferromagnetic (AFM) orderings along a predefined path (which were almost degenerate); their energy-volume common-tangent gave coexistence P_0 at 10.5 GPa.[24]

III. PRESENT RESULTS

To determine P_0 of equilibrium coexistence of FM bcc and NM hcp phases, we calculate volume V, energy E, and enthalpy $H = E+PV$ (Fig. 2) at various hydrostatic external pressures P. Each unit cell is fully relaxed at a given P. All atomic forces and all non-diagonal pressure components remain zero due to symmetry. Diagonal pressure components are the same by symmetry in bcc and fcc phases, while their difference does not exceed 0.03 GPa in hcp. Magnetization of the FM bcc reduces with pressure and collapses to zero at ≈900 GPa; hcp magnetization is set to zero at all pressures.

The slope of the common tangent to the $E(V)$ curves in Fig. 2a gives P_0 of 8.4 GPa; this pressure gives zero enthalpy difference in Fig. 2c, and is compared to all experiments in Fig. 2d. The previously calculated values of 13.1 GPa[19] and 10.5 GPa[24] do not agree with all the experimental data, summarized in Table I and Fig. 2d.

To obtain these results, we used the Vienna ab initio simulation package (VASP)[187–189] with generalized gradient approximation (GGA)[190,191] and projector augmented-wave (PAW) potentials.[192,193] We use 334.88 eV energy cutoff for the plane-wave basis with augmentation charge cutoff of 511.4 eV. The modified Broyden method[194] is used for self-consistency. We carefully check

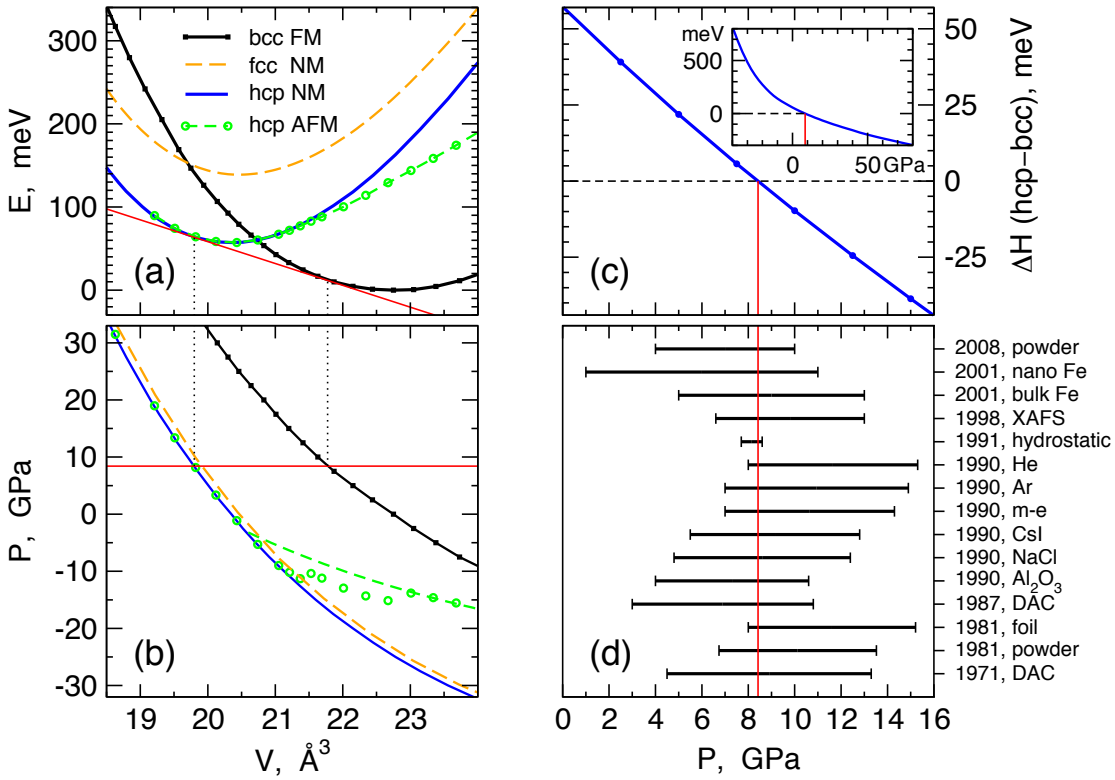

FIG. 2: (a) Energy [meV/atom] relative to bcc at 0 GPa and (b) pressure [GPa] versus volume [Å^3/cell] for hydrostatically relaxed 2-atom unit cells of bcc FM (black), hcp NM (blue) and AFM (green), and fcc NM iron (orange); with DFT values (dots) and least-squares fit to the Birch-Murnaghan EoS (lines). Common tangent construction (red line) yields $P_0 = 8.42$ GPa. Vertical dotted lines are guides to the eye. (c) Enthalpy difference [meV/Fe] between hcp and bcc phases versus pressure [GPa] (inset shows a larger range). (d) Comparison of the calculated $P_0 = 8.42$ GPa (vertical red line) with experimental data from Table I, represented by $[P_{end}^{\varepsilon\to\alpha} - P_{start}^{\alpha\to\varepsilon}]$ horizontal segments. Except for the 1991 hydrostatic experiment,[9] most diamond anvil cells[3,6] provided uniaxial or highly anisotropic pressure.

convergence with respect to the number of k-points (up to 32^3=32768) in the Γ-centered Monkhorst-Pack[195] mesh within the tetrahedron method with Blöchl corrections. Gaussian smearing with $\sigma = 0.05$ eV with 16^3=4096 k-points in the 2-atom cell is used for relaxation.

The role of the exchange correlation functional V_{xc} is well discussed in the literature.[25,206] Previous failure of the LDA to properly describe the Fe ground state was an impetus in developing the GGA,[190,191] which we use. We rely on decades of DFT testing, and appearance of the calculated value of P_0 within the rather narrow range (1) is another success of GGA[190,191] for iron. Using a less accurate V_{xc} could shift the calculated P_0 by a few GPa, while the GGA is claimed to provide one of the most accurate results for the relative structural energies in iron.[207] We use PBE-PAW-GGA to provide reasonable agreement with experiment for the lattice constants, compressibilities, and energies. The expected systematic errors in the equilibrium lattice constants $\varepsilon(a) \leq 1\%$, volume $\varepsilon(V) = [\varepsilon(a)]^3 \leq 3\%$, and relative energies $\delta E \leq 1$ meV/atom give an estimate of the error in P_0 not exceeding 0.5 GPa.

There are many EoS for solids.[196] We fit our $E(V)$ data in Fig. 2a to the Birch-Murnaghan EoS.[197,198] For iron, the parameters are given in Table 2 for FM bcc at low pressure, and NM hcp at high pressure. Although hcp at lower pressure and density ($V > 23$ Å^3/cell) changes from NM to AFM, their $E(V)$ curves at $V < 21$ Å^3 are almost degenerate. These values have some dependence on the range of fitted data, and are affected by the EoS functional form. As expected, calculated volume V_0 is reduced by 3% compared to experiment due to the standard DFT systematic error (i.e., 1% in lattice constants). This DFT error introduces a systematic 3% error (0.25 GPa) in our bcc-hcp coexistence pressure.

Our result for bcc iron is in agreement with the previous DFT calculations,[25,199,200] with B_0 ranging from 171 to 194 GPa from EMTO, VASP, and Wien2K codes, which compare well with the assesses values of 159–206 GPa.[201–203] Due to their pressure and temperature dependence, the assessed elastic constants and EoS parameters depend on the fitting procedure. The measured by inelastic neutron scattering at 300 K bulk modulus $B = C_{11} - \frac{4}{3}C'$ changes from 159 GPa at zero pressure to 206 GPa at $P = 9.8$ GPa.[203] Our EoS coefficients for the hcp single crystal agree with previously calculated

Fe phase	V_0		B_0	B_0'
	$\frac{\text{Å}^3}{\text{cell}}$	$\frac{\text{cm}^3}{\text{mol}}$	GPa	
bcc FM	22.72	6.84	185	4.7
bcc expt.[201]	23.56	7.09	172	5.0
bcc expts.			159–206	
hcp NM	20.34	6.13	293	4.5
hcp AFM	19.94	6.004	140	3.9
hcp expt.[82]	22.35	6.73	167	5.8
hcp expts.			156–195	4–6

TABLE II: Birch-Murnaghan EoS parameters, assessed or extrapolated from theory and experiment. Values depend on data, its P and T range, and fitting procedure, see text.

ones[204,205] at T=0 K, summarized in Table 1 in Ref. 204. However, the experimentally assessed EoS for the hcp martensite[82,208] with B_0 of 156–195 GPa and B_0' of 4.3–5.8 differs from that calculated for a hcp single crystal (Table II). This difference is expected because a martensite is a composite with both compressed and dilated regions, and any non-homogeneous distortion increases energy, shifting up and distorting the $E(V)$ curve in Fig. 2a. We note that although the fitted values of B_0 (293 and 140 GPa in Table 2) differ quite dramatically for the hcp NM and AFM curves due to their divergence at larger V and lower pressures, these curves coincide near P_0 and their tangent is the same in Fig. 2a.

In addition, we use the generalized solid-state nudged elastic band (GSS-NEB) method[184,185] to find the transformation path at P_0 within the shear-shuffle model,[6] see Fig. 3. Enthalpy of the transition state (TS) is 156 meV/Fe above the bcc and hcp, which have the same enthalpy at P_0. Coherent coexistence of the magnetic and non-magnetic states with the same atomic and cell degrees of freedom at the TS, which has a form of a cusp, causes a coherency stress, related to the 25 GPa discontinuity in the internal pressure in Fig. 3. The electronic interactions propagate with the speed of light, while pressure propagates with the speed of sound. Hence, electronic transitions (causing discontinuity in magnetization in Fig. 3) happen faster than the structural transformation (resulting in continuous volume, shuffle and shear change within the GSS-NEB method) during the magneto-structural transformation of iron under pressure. To state it briefly, change of density (or unit cell volume V) causes transformation of the magnetic state and a discontinuous change of magnetization M, which creates a discontinuous change of the internal pressure P, which pushes further adjustment of the volume; the causality is $V \to M \to P \to V$.

Due to an energy barrier (Fig. 3), there is a hysteresis, and the forward $\alpha \to \varepsilon$ transformation starts at a higher pressure than P_0. The austenitic bcc α phase has a chance of being isotropic at hydrostatic pressure. However, the anisotropic hcp ε-phase forms a martensite, which has non-hydrostatic internal stress in experiment; due to the difference between hexagonal a and c directions it is not isotropic at the microscale. Only when this phase disappears, one can make a comparison between theoretical and experimental hydrostatic pressure.

A question remains: "Why should a common-tangent construction for the ideal relaxed structure be relevant to experiments at all?" In Fig. 2a we deal with energies of the ideal relaxed structures at hydrostatic pressure, while there are imperfections in experiments. At any hydrostatic pressure P, energy of the relaxed ideal structure is the lowest; defects and non-hydrostaticity effects shift it up, and we can predict the consequence of this shift for direct $\alpha \to \varepsilon$ transformation. Martensite has more structural defects and anisotropy compared to austenite, giving a larger systematic upward shift for the hcp phase of the energy curves in Fig. 2a and a larger slope (higher pressure) for the common-tangent. In addition to an energy barrier, this effect partially explains a tendency towards higher $P_{start}^{\alpha\to\varepsilon}$ values in less hydrostatic experiments (Fig. 2d). Again, a martensite has anisotropic martensitic pressure (up to 25 GPa from Fig. 3), hence one can deal with a hydrostatic pressure only after complete disappearance of the martensitic phase, which is why $P_{end}^{\varepsilon\to\alpha}$ brackets P_0 in (1) on the lower side. The enthalpy barrier (Fig. 3) is responsible for the fact of the hysteresis, and a variety of structural defects and non-hydrostatic contributions in experiments accounts for the scatter of experimental data (Fig. 2d). We emphasize the import of (1) for comparing an ideal value of P_0 to all experiments.

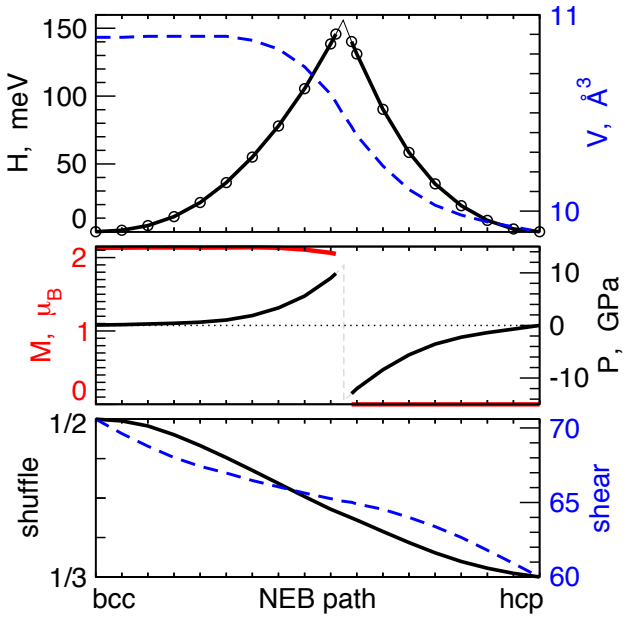

FIG. 3: Enthalpy H, volume V, magnetization M [per atom], internal pressure P, atomic shuffle [defined as direct coordinate of the second atom in a 2-atom unit cell relative to the first atom placed at zero], and shear angle [degrees] at P_0 versus the GSS-NEB path from bcc to hcp.

IV. DISCUSSION

Iron: Transformation from α (bcc) to ε (hcp) iron is martensitic,[3] and the hysteresis loop can be characterized by four pressures: $P_{start}^{\alpha\to\varepsilon}$, $P_{end}^{\alpha\to\varepsilon}$, $P_{start}^{\varepsilon\to\alpha}$, and $P_{end}^{\alpha\to\varepsilon}$. In experiment,[6,7] ε-phase appears at $P_{start}^{\alpha\to\varepsilon}$ between 8.6 and 15.3 GPa, while α-phase is fully converted above $P_{end}^{\alpha\to\varepsilon}$ between 14 and 25 GPa upon loading. Whereas, upon unloading, α-phase appears at $P_{start}^{\varepsilon\to\alpha}$ between 16 and 7 GPa and ε-phase disappears below $P_{end}^{\varepsilon\to\alpha}$ between 8 and 1 GPa. Importantly, there is no strict inequality between $P_{start}^{\alpha\to\varepsilon}$ and $P_{start}^{\varepsilon\to\alpha}$ due to the martensitic stress distribution in the ε-phase.

Our calculated P_0 of 8.4 GPa is below $P_{start}^{\alpha\to\varepsilon}$ and above $P_{end}^{\varepsilon\to\alpha}$, see inequality (1). It agrees well with the experimental distribution of $P_{start}^{\alpha\to\varepsilon} \geq 8.6$ GPa and $P_{end}^{\varepsilon\to\alpha} \leq 8.5$ GPa. The observed $P_{start}^{\varepsilon\to\alpha}$ and $P_{end}^{\alpha\to\varepsilon}$ are highly affected by the martensitic stress within the hcp ε-phase. A martensitic transformation occurs between an isotropic (bcc) austenite and an anisotropic (hcp) martensite, which experience martensitic stress resulting in anisotropic distortions. In other words, there is little internal stress in austenite and large anisotropic internal stresses in martensite. However, martensitic stress is not taken into account in our calculation of the bcc-hcp equilibrium coexistence pressure P_0. Because hcp does not exist below $P_{start}^{\alpha\to\varepsilon}$ and $P_{end}^{\varepsilon\to\alpha}$, these values should not be affected by the martensitic stress in hcp (though the transformation can be delayed due to an energy barrier), and can be used in the proper comparison to experiment. Hence, P_0 must be between $P_{start}^{\alpha\to\varepsilon}$ and $P_{end}^{\varepsilon\to\alpha}$, see inequality (1). These experimental ranges are compared with our calculated value of P_0 in Fig. 2d, with an excellent agreement between theory and experiment.

In Fig. 3 we present the energy barrier and the transition state at P_0 via a generalized solid-solid nudged-elastic band[184] method that incorporates magnetization and volume collapse. Change of magnetization of the TS from FM to NM results in the pressure change by $\Delta P = 25$ GPa. This calculated ΔP at the TS agrees with the observed bcc-hcp coexistence interval $[P_{end}^{\varepsilon\to\alpha}, P_{end}^{\alpha\to\varepsilon}]$.

Lithium: To illustrate further the generality of inequality (1), we apply it to the pressure-induced transformation in fcc (isotropic austenite) lithium (99.9% ^{7}Li) to the intermediate hR1 (rhombohedral) phase near 39 GPa.[209,210] The hR1 structure with 1 atom/cell is a 7% distortion of fcc along a cubic axis; it can form a martensite due to axial anisotropy. At 180 K and increasing P in a DAC under inert gas,[210] the structure remains fcc up to 38.3 GPa; a new set of XRD intense diffraction lines appears at $P_{start}^{bcc\to hR1} = 39.8$ GPa (and disappears at $P_{end}^{hR1\to cI16} = 42.5$ GPa), thus providing an upper bound for $P_0 < P_{start}^{bcc\to hR1}$. Higher values for the upper bound are provided by dynamic shock compression experiments,[209] which measure a sharp increase of resistivity at $P_{start}^{bcc\to other} = 42$ GPa (isoentropic compression from 77K) or 43 GPa (multistep shock at $T < 660$ K); the other phase was not identified. A comparable upper bound is offered by the DAC experiment[211] at 25 K, which found a small resistivity drop at $P_{start}^{bcc\to other} = 42$ GPa upon loading (attributed to transitions from fcc to hR1 and from hR1 to cI16). Interestingly, no change is observed in the Raman spectra at these pressures.[212] While compression data provides $P_{start}^{bcc\to hR1}$ as an upper bound of P_0 for the fcc→hR1, more decompression measurements are needed to determine the lower bound of $P_0(T)$ using inequality (1).

Solid structures of Li at P from 5 to 130 GPa and T from 77 to 300K were identified by XRD in DAC[213] using multiple $P-T$ paths; hR1 phase was detected around 40 GPa at $T \leq 200$ K (with measurement errors of ± 2 GPa and ± 10 K). We emphasize expectation of a hysteresis for the fcc–hR1 transformation, which might be martensitic. Due to the hysteresis, current structure depends not only on the instant P and T values, but also on the path (history), and should be represented by a directed arrow (not just a dot) on the $P-T$ diagram (e.g., Fig. 1 in Ref. 213).

V. SUMMARY

We presented and explored a methodology for comparing idealistic theoretical predictions at hydrostatic pressure to realistic experiments with anisotropic stress, based on inequality 1. Due to its importance, we revisited the iron bcc-hcp equilibrium coexistence; our calculated pressure of 8.4 ± 0.5 GPa is in agreement with available experimental data. Anisotropic internal stress in the hcp martensite, difference in volume between FM bcc and NM (and competing AFM) hcp iron near the transition state contribute to the spread of the experimentally assessed (non-equilibrium) bcc-hcp coexistence pressures, as well as to the uncertainty in the equation of state of hcp martensite. We emphasized the difference between a single crystal and a martensite and improved understanding of the available data for iron under pressure. Importantly, we suggested a universal inequality (1), graphically illustrated in Fig. 2d, for proper comparison of the assessed and calculated pressures characterizing first-order transitions in many materials, in particular the martensitic transformations in solids, as shown for iron and lithium.

Acknowledgments

We thank Graeme Henkelman, Paul Canfield, and Iver Anderson for discussion. This work was supported by the U.S. Department of Energy (DOE), Office of Science, Basic Energy Sciences (BES), Materials Science and Engineering Division. This research was performed at the Ames Laboratory, which is operated for the U.S. DOE by Iowa State University under contract DE-AC02-07CH11358.

References

* Electronic address: zarkev@ameslab.gov;ddj@ameslab.gov

[1] D. Bancroft, E. L. Peterson, and S. Minshall, J. Appl. Phys. 27, 291 (1956).

[2] A. S. Balchan and H. G. Drickamer, Rev. Sci. Instrum. 32, 308 (1961).

[3] P. M. Giles, M. H. Longenbach, and A. R. Marder, J. Appl. Phys. 42, 4290 (1971).

[4] G. Zou, P. M. Bell, and H. K. Mao, in Year Book (Carnegie Institute of Washington, BookCrafters, Inc., Chelsea, Michigan, 1980-1981), Vol. 80, p. 272.

[5] H. K. Mao, W. A. Bassett, and T. Takahashi, J. Appl. Phys. 38, 272 (1967).

[6] W. A. Bassett and E. Huang, Science 238, 780 (1987).

[7] R. Boehler, N. Vonbargen, and A. Chopelas, J. Geophys. Res. 95 (B13), 21731 (1990).

[8] N. B. von Bargen, R. Boehler, High Pressure Res. 6, 133 (1990).

[9] R. D. Taylor, M. P. Pasternak, and R. Jeanloz, J. Appl. Phys. 69, 6126 (1991).

[10] F. Wang, R. Ingalls, and E. D. Crozier, Jpn. J. Appl. Phys. 32, Suppl. 32-2, 749 (1993).

[11] F. M. Wang and R. Ingalls, Phys. Rev. B 57, 5647 (1998).

[12] J. Z. Jiang, J. S. Olsen, and L. Gerward, Mater. Trans. 42, 1571 (2001).

[13] F. Baudelet, S. Pascarelli, O. Mathon, J. P. Itie, A. Polian, M. d' Astuto, and J. C. Chervin, J. Phys.: Condens. Matter 17, S957 (2005).

[14] L. Miyagi, M. Kunz, J. Knight, J. Nasiatka, M. Voltolini, and H. R. Wenk, J. Appl. Phys. 104 (2008).

[15] B. Yaakobi, T. R. Boehly, D. D. Meyerhofer, T. J. B. Collins, B. A. Remington, P. G. Allen, S. M. Pollaine, H. E. Lorenzana, and J. H. Eggert, Phys. Rev. Lett. 95, 075501 (2005).

[16] J. Jung, M. Fricke, G. Hampel, and J. Hesse, Hyperfine Interact. 72, 375 (1992).

[17] M. Ekman, B. Sadigh, K. Einarsdotter, and P. Blaha, Phys. Rev. B 58, 5296 (1998).

[18] M. Sob, M. Friak, L. G. Wang, and V. Vitek, Multiscale Modelling of Materials 538, 523 (1999).

[19] D. F. Johnson and E. A. Carter, J. Chem. Phys. 128, 104703 (2008).

[20] J. B. Liu and D. D. Johnson, Phys. Rev. B 79, 134113 (2009).

[21] J. L. Shao, A. M. He, S. Q. Duan, P. Wang, and C. S. Qin, Acta Phys Sin-Ch Ed 59, 4888 (2010).

[22] B. T. Wang, J. L. Shao, G. C. Zhang, W. D. Li, and P. Zhang, J. Phys.: Condens. Matter 21, 495702 (2009).

[23] B. T. Wang, J. L. Shao, G. C. Zhang, W. D. Li, and P. Zhang, J. Phys.: Condens. Matter 22, 435404 (2010).

[24] M. Friak and M. Sob, Phys. Rev. B 77, 174117 (2008).

[25] L. Vocadlo, G. A. de Wijs, G. Kresse, M. Gillan, and G. D. Price, Faraday Discuss. 106, 205–218 (1997).

[26] K. J. Caspersen, A. Lew, M. Ortiz, and E. A. Carter, Phys. Rev. Lett. 93, 115501 (2004).

[27] N. Suzuki, T. Souraku, I. Hamada, and T. Takezawa, High Pressure Res. 22, 451 (2002).

[28] L. Stixrude and R. E. Cohen, High-Pressure Science and Technology - 1993, Parts 1 and 2, 911 (1994).

[29] V. Potapkin, C. McCammon, K. Glazyrin, A. Kantor, I. Kupenko, C. Prescher, R. Sinmyo, G.V. Smirnov, A.I. Chumakov, R. Rüffer, L. Dubrovinsky, Nat. Commun. 4, 1427 (2013).

[30] M. Pozzo, C. Davies, D. Gubbins, and D. Alfé, Nature 485, 355 (2012).

[31] D. Andrault, S. Petitgirard, G. Lo Nigro, J. L. Devidal, G. Veronesi, G. Garbarino, and M. Mezouar, Nature 487, 354 (2012).

[32] R. Nomura, H. Ozawa, S. Tateno, K. Hirose, J. Hernlund, S. Muto, H. Ishii, and N. Hiraoka, Nature 473, 199 (2011).

[33] J. R. Rustad and Q. Z. Yin, Nat. Geosci. 2, 514 (2009).

[34] J. F. Lin, V. V. Struzhkin, S. D. Jacobsen, M. Y. Hu, P. Chow, J. Kung, H. Z. Liu, H. K. Mao, and R. J. Hemley, Nature 436, 377 (2005).

[35] J. H. Nguyen and N. C. Holmes, Nature 427, 339 (2004).

[36] D. J. Frost, C. Liebske, F. Langenhorst, C. A. McCammon, R. G. Tronnes, and D. C. Rubie, Nature 428, 409 (2004).

[37] L. Vocadlo, D. Alfé, M. J. Gillan, I. G. Wood, J. P. Brodholt, and G. D. Price, Nature 424, 536 (2003).

[38] L. Dubrovinsky et al., Nature 422, 58 (2003).

[39] L. Dubrovinsky et al., Science 316, 1880 (2007).

[40] A. B. Belonoshko, R. Ahuja, and B. Johansson, Nature 424, 1032 (2003).

[41] A. B. Belonoshko, N. V. Skorodumova, A. Rosengren, B. Johansson, Science 319, 797 (2008).

[42] G. Steinle-Neumann, L. Stixrude, R. E. Cohen, and O. Gulseren, Nature 413, 57 (2001).

[43] H. R. Wenk, S. Matthies, R. J. Hemley, H. K. Mao, and J. Shu, Nature 405, 1044 (2000).

[44] S. C. Singh and J. P. Montagner, Nature 400, 629 (1999).

[45] H. K. Mao, J. F. Shu, G. Y. Shen, R. J. Hemley, B. S. Li, and A. K. Singh, Nature 399, 280 (1999).

[46] D. Alfé, M. J. Gillan, and G. D. Price, Nature 401, 462 (1999).

[47] H. K. Mao, J. F. Shu, G. Y. Shen, R. J. Hemley, B. S. Li, and A. K. Singh, Nature 396, 741 (1998).

[48] G. A. de Wijs, G. Kresse, L. Vocadlo, D. Dobson, D. Alfé, M. J. Gillan, and G. D. Price, Nature 392, 805 (1998).

[49] D. P. Summers and S. Chang, Nature 365, 630 (1993).

[50] A. Jephcoat and P. Olson, Nature 325, 332 (1987).

[51] Y. Fukai, Nature 308, 174 (1984).

[52] S. Anzellini, A. Dewaele, M. Mezouar, P. Loubeyre, and G. Morard, Science 340, 464 (2013).

[53] A. S. Cote, L. Vocadlo, and J. P. Brodholt, Earth Planet. Sci. Lett. 345, 126 (2012).

[54] S. Tateno, K. Hirose, Y. Ohishi, and Y. Tatsumi, Science 330, 359 (2010).

[55] W. Luo, B. Johansson, O. Eriksson, S. Arapan, P. Souvatzis, M. I. Katsnelson, and R. Ahuja, Proc. Natl. Acad. Sci. USA 107, 9962 (2010).

[56] T. Irifune, T. Shinmei, C. A. McCammon, N. Miyajima, D. C. Rubie, and D. J. Frost, Science 327, 193 (2010).

[57] X. L. Sun and X. D. Song, Earth Planet. Sci. Lett. 269,

56 (2008).
[58] Y. Kuwayama, K. Hirose, N. Sata, and Y. Ohishi, Earth Planet. Sci. Lett. 273, 379 (2008).
[59] B. Chen, L. L. Gao, K. Funakoshi, and J. Li, Proc. Natl. Acad. Sci. USA 104 (22), 9162 (2007).
[60] P. Modak, A. K. Verma, R. S. Rao, B. K. Godwal, and R. Jeanloz, J. Mater. Sci. 41, 1523 (2006).
[61] S. Speziale, A. Milner, V. E. Lee, S. M. Clark, M. P. Pasternak, and R. Jeanloz, Proc. Natl. Acad. Sci. USA 102, 17918 (2005).
[62] J. Badro, G. Fiquet, F. Guyot, J. P. Rueff, V. V. Struzhkin, G. Vanko, and G. Monaco, Science 300, 789 (2003).
[63] J. F. Lin, D. L. Heinz, A. J. Campbell, J. M. Devine, and G. Y. Shen, Science 295, 313 (2002).
[64] S. Merkel, A. F. Goncharov, H. K. Mao, P. Gillet, and R. J. Hemley, Science 288, 1626 (2000).
[65] A. Laio, S. Bernard, G. L. Chiarotti, S. Scandolo, and E. Tosatti, Science 287, 1027 (2000).
[66] T. Okuchi, Science 278, 1781 (1997).
[67] C. S. Yoo, J. Akella, A. J. Campbell, H. K. Mao, and R. J. Hemley, Science 270, 1473 (1995).
[68] F. Birch, Am. J. Sci. 238, 192 (1940).
[69] L. Stixrude and R. E. Cohen, Science 267, 1972 (1995).
[70] L. V. Pourovskii, T. Miyake, S. I. Simak, A. V. Ruban, L. Dubrovinsky, and I. A. Abrikosov, Phys. Rev. B 87, 115130 (2013).
[71] B. Martorell, J. Brodholt, I. G. Wood, and L. Vocadlo, Earth Planet. Sci. Lett. 365, 143 (2013).
[72] K. A. Evans, T. C. McCuaig, D. Leach, T. Angerer, and S. G. Hagemann, Geology 41, 99 (2013).
[73] A. M. Mloszewska, E. Pecoits, N. L. Cates, S. J. Mojzsis, J. O'Neil, L. J. Robbins, and K. O. Konhauser, Earth Planet. Sci. Lett. 317, 331 (2012).
[74] Y. N. Wu, D. M. Wang, and Y. S. Huang, AIP Advances 1, 032122 (2011).
[75] K. G. Taylor and K. O. Konhauser, Elements 7, 83 (2011).
[76] M. Tamura, J. Japan Inst. Metals 75 (1), 1–4 (2011).
[77] J. Persson, C. Desgranges, and J. Delhommelle, Chem. Phys. Lett. 511, 57 (2011). doi: 10.1016/j.cplett.2011.06.018
[78] O. Narygina, L. S. Dubrovinsky, C. A. McCammon, A. Kurnosov, I. Y. Kantor, V. B. Prakapenka, and N. A. Dubrovinskaia, Earth Planet Sci. Lett. 307, 409 (2011).
[79] Z. Mao, J. F. Lin, H. P. Scott, H. C. Watson, V. B. Prakapenka, Y. Xiao, P. Chow, and C. McCammon, Earth Planet Sci. Lett. 309, 179 (2011).
[80] T. Ishikawa, T. Tsuchiya, and J. Tsuchiya, Phys. Rev. B 83, 212101 (2011).
[81] T. Komabayashi and Y. W. Fei, J. Geophys. Res. 115, B03202 (2010).
[82] L. S. Dubrovinsky, S. K. Saxena, F. Tutti, S. Rekhi, and T. Le Behan, Phys. Rev. Lett. 84, 1720 (2000).
[83] L. Dubrovinsky, J. F. Lin, and N. Dubrovinskaia, "Mineral physics of Earth core: iron alloys at extreme condition," in "High-Pressure Crystallography," p. 35 (Springer, 2010). doi: 10.1007/978-90-481-9258-8_4.
[84] A. S. Cote, L. Vocadlo, D. P. Dobson, D. Alfé, and J. P. Brodholt, Phys. Earth Planet. In. 178, 2 (2010).
[85] L. Koci, A. B. Belonoshko, and R. Ahuja, Geophys. J. Int. 168, 890 (2007).
[86] A. B. Belonoshko and A. Rosengren, Geochim. Cosmochim. Ac. 74, A75 (2010).
[87] A. B. Belonoshko, T. Bryk, and A. Rosengren, Phys. Rev. Lett. 104, 245703 (2010).
[88] H. Asanuma, E. Ohtani, T. Sakai, H. Terasaki, S. Kamada, T. Kondo, and T. Kikegawa, Phys. Chem. Minerals 37, 353 (2010).
[89] D. Alfé, Rev. Mineral. Geochem. 71, 337 (2010).
[90] M. Walter, O. Lord, G. Helffrich, and D. Walker, Geochim. Cosmochim. Ac. 73, A1405 (2009).
[91] E. Sola, J. P. Brodholt, and D. Alfé, Phys. Rev. B 79, 024107 (2009).
[92] E. Sola and D. Alfé, Phys. Rev. Lett. 103, 078501 (2009).
[93] D. E. Smylie, V. V. Brazhkin, and A. Palmer, Phys-Usp+ 52, 79 (2009).
[94] K. Kadas, L. Vitos, B. Johansson, and R. Ahuja, Proc. Natl. Acad. Sci. USA 106, 15560 (2009).
[95] T. Ishikawa, J. Tsuchiya, and T. Tsuchiya, Geochim. Cosmochim. Ac. 73, A573 (2009).
[96] D. Alfé, Phys. Rev. B 79, 060101R (2009).
[97] M. Mattesini, E. Buforn, A. Udias, L. Vitos, and R. Ahuja, High Pressure Res. 28, 437 (2008).
[98] J. F. Lin and T. Tsuchiya, Phys. Earth Planet. In. 170, 248 (2008).
[99] Y. H. Li, K. J. Hou, and D. F. Wan, Geochim. Cosmochim. Ac. 72, A548 (2008).
[100] J. Li, L. Gao, B. Chen, E. Alp, J. Zhao, and K. Hirose, Geochim. Cosmochim. Ac. 72, A541 (2008).
[101] K. Kadas, L. Vitos, and R. Ahuja, Earth Planet. Sci. Lett. 271, 221 (2008).
[102] G. J. Golabek, H. Schmeling, and P. J. Tackley, Earth Planet. Sci. Lett. 271, 24 (2008).
[103] A. S. Cote, L. Vocadlo, and J. P. Brodholt, J. Phys. Chem. Solids 69, 2177 (2008).
[104] D. K. Belashchenko, N. E. Kravchunovskaya, and O. I. Ostrovski, Inorganic Materials 44, 248 (2008).
[105] A. K. Singh, Phys. Earth Planet. In. 164, 75 (2007).
[106] K. Shigemori, D. Ichinose, T. Irifune, K. Otani, T. Shiota, T. Sakaiya, and H. Azechi, Eur. Phys. J. D 44, 301 (2007).
[107] P. Modak, A. K. Verma, R. S. Rao, B. K. Godwal, L. Stixrude, and R. Jeanloz, J. Phys.: Condens. Matter 19 (2007).
[108] M. A. Bouhifd, L. Gautron, N. Bolfan-Casanova, V. Malavergne, T. Hammouda, D. Andrault, and A. P. Jephcoat, Phys. Earth Planet. In. 160, 22 (2007).
[109] J. Badro, G. Fiquet, F. Guyot, E. Gregoryanz, F. Occelli, D. Antonangeli, and M. d'Astuto, Earth Planet. Sci. Lett. 254, 233 (2007).
[110] F. W. Zhang and A. R. Oganov, Earth Planet. Sci. Lett. 249, 436 (2006).
[111] K. Shigemori, D. Ichinose, T. Irifune, K. Otani, T. Shiota, T. Sakaiya, and H. Azechi, J. Phys. IV France 133, 37–41 (2006). doi: 10.1051/jp4:2006133008
[112] K. Shigemori, A. Ichinose, T. Irifune, K. Otani, T. Shiota, T. Sakaiya, and H. Azechi, Shock Compression of Condensed Matter, Parts 1 and 2, 845, 1480 (2006).
[113] K. K. M. Lee and G. Steinle-Neumann, J. Geophys. Res. 111 (2006).
[114] J. Badro, G. Fiquet, and F. Guyot, Geochim. Cosmochim. Ac. 70, A28 (2006).
[115] W. Sturhahn, J. M. Jackson, and J. F. Lin, Geophys. Res. Lett. 32 (2005).
[116] G. Schmidt, H. Palme, and K. L. Kratz, Meteorit. Planet. Sci. 40, A135 (2005).
[117] V. N. Mineev and A. I. Funtikov, Izvestiya, Phys. Solid Earth (Fizika Zemli) 41, 539 (2005).
[118] J. F. Lin, V. V. Struzhkin, S. D. Jacobsen, G. Y. Shen,

V. B. Prakapenka, H. K. Mao, and R. J. Hemley, J. Synchrotron Radiat. 12, 637 (2005).
[119] C. M. S. Gannarelli, D. Alfé, and M. J. Gillan, Phys. Earth Planet. In. 152, 67 (2005).
[120] S. Weyer, A. Woodland, C. Munker, G. L. Arnold, R. Chakrabarti, and A. D. Anbar, Geochim. Cosmochim. Ac. 68, A736 (2004).
[121] J. Shanker, B. P. Singh, and S. K. Srivastava, Phys. Earth Planet. In. 147, 333 (2004).
[122] Y. Z. Ma, M. Somayazulu, G. Y. Shen, H. K. Mao, J. F. Shu, and R. J. Hemley, Phys. Earth Planet. In. 143, 455 (2004).
[123] K. K. M. Lee, G. Steinle-Neumann, and R. Jeanloz, Geophys. Res. Lett. 31 (2004).
[124] N. Hirao, T. Kondo, E. Ohtani, K. Takemura, and T. Kikegawa, Geophys. Res. Lett. 31 (2004).
[125] D. J. Frost, C. Liebske, C. A. McCammon, F. Langenhorst, R. Tronnes, and D. C. Rubie, Lithos 73, S38 (2004).
[126] Y. Kato, Geochim. Cosmochim. Ac. 67, A204 (2003).
[127] C. M. Johnson, B. L. Beard, N. J. Beukes, C. Klein, and J. M. O'Leary, Contrib. Mineral. Petrol. 144, 523 (2003).
[128] G. E. Grechnev, R. Ahuja, and O. Eriksson, Phys. Rev. B 68, 064414 (2003).
[129] B. L. Beard, C. M. Johnson, K. L. Von Damm, and R. L. Poulson, Geology 31, 629 (2003).
[130] Y. Wang, R. Ahuja, and B. Johansson, J. Phys.-Condens. Mat. 14, 7321 (2002).
[131] Y. Wang, R. Ahuja, and B. Johansson, Phys. Rev. B 65, 014104 (2001).
[132] J. F. Lin, D. L. Heinz, A. J. Campbell, J. M. Devine, W. L. Mao, and G. Y. Shen, Geophys. Res. Lett. 29 (2002).
[133] B. L. Beard, C. M. Johnson, and K. L. Von Damm, Geochim. Cosmochim. Ac. 66, A58 (2002).
[134] D. Alfé, G. D. Price, and M. J. Gillan, Phys. Rev. B 65, 165118 (2002).
[135] C. Yapp, Annu. Rev. Earth Pl. Sc. 29, 165 (2001).
[136] R. J. Hemley and H. K. Mao, Int. Geol. Rev. 43, 1–26 (2001).
[137] A. I. Funtikov, Izvestiya, Phys. Solid Earth (Fizika Zemli) 37, 703 (2001).
[138] D. Alfé, G. D. Price, and M. J. Gillan, Phys. Rev. B 64, 045123 (2001).
[139] Y. G. Zhang and G. J. Guo, Phys. Earth Planet. In. 122, 289 (2000).
[140] I. Jackson, J. D. Fitz Gerald, and H. Kokkonen, J. Geophys. Res. 105, 23605 (2000).
[141] A. I. Funtikov, Izvestiya, Phys. Solid Earth [Fizika Zemli] 36, 958 (2000).
[142] D. Alfé, G. Kresse, and M. J. Gillan, Phys. Rev. B 61, 132 (2000).
[143] L. Vocadlo, J. Brodholt, D. Alfé, G. D. Price, and M. J. Gillan, Geophys. Res. Lett. 26, 1231 (1999).
[144] J. P. Poirier and G. D. Price, Phys. Earth Planet. In. 110, 147 (1999).
[145] L. Stixrude, E. Wasserman, and R. E. Cohen, Geophysical Monograph Series 101, 159 (1998).
[146] T. Okuchi, J. Phys.: Condens. Matter 10, 11595 (1998).
[147] F. Guyot, J. H. Zhang, I. Martinez, J. Matas, Y. Ricard, and M. Javoy, Eur J Mineral 9, 277 (1997).
[148] P. Soderlind, J. A. Moriarty, and J. M. Wills, Phys. Rev. B 53, 14063 (1996).
[149] J. P. Poirier, A. Goddat, and J. Peyronneau, Philos T R Soc A 354, 1361 (1996).
[150] I. Suzuki, et al., High-Pressure Science and Technology – 1993, Pts. 1 and 2, 935 (1994).
[151] C. S. Yoo, N. C. Holmes, M. Ross, D. J. Webb, and C. Pike, Phys. Rev. Lett. 70, 3931 (1993).
[152] Y. Hirayama, T. Fujii, and K. Kurita, Geophys. Res. Lett. 20, 2095 (1993).
[153] M. Ross, D. A. Young, and R. Grover, J. Geophys. Res. 95, 21713 (1990).
[154] D. A. Boness and J. M. Brown, J. Geophys. Res. 95, 21721 (1990).
[155] O. L. Anderson, J. Geophys. Res. 95, 21697 (1990).
[156] D. A. Boness, J. M. Brown, and A. K. Mcmahan, Phys. Earth Planet. In. 42, 227 (1986).
[157] I. S. Kulikov, Izv. Akad. Nauk SSSR, Metally [Russ. Metall.], 6, 9–15 (1985).
[158] V. K. Levashov and B. V. Oleinikov, Dokl. Akad. Nauk SSSR 278, 719 (1984).
[159] V. N. Zharkov, Dokl. Akad. Nauk SSSR 135, 1378 (1960).
[160] B. P. Krotov, Dokl. Akad. Nauk SSSR 121, 326 (1958).
[161] W. Westphal, Naturwissenschaften 10, 260 (1922).
[162] E. Wilson, P. Roy. Soc. Lond. A Mat. 90, 179 (1914).
[163] J. J. Yang, J. I. Goldstein, and E. R. D. Scott, Nature 446, 888 (2007).
[164] F. Paneth, W. D. Urry, and W. Koeck, Nature 125, 490–491 (1930).
[165] M. I. Oshtrakh, M. Y. Larionov, V. I. Grokhovsky, and V. A. Semionkin, Meteorit. Planet. Sci. 47, A305 (2012).
[166] L. V. Agafonov, V. A. Popov, G. N. Anoshin, L. N. Pospelova, V. I. Zabelin, and V. I. Kudryavtsev, Russ. Geol. Geophys. 52, 620 (2011).
[167] M. I. Oshtrakh, M. Y. Larionov, V. I. Grokhovsky, and V. A. Semionkin, Mater. Chem. Phys. 130, 373 (2011).
[168] M. I. Oshtrakh, V. I. Grokhovsky, N. V. Abramova, V. A. Semionkin, and O. B. Milder, Isiame 2008, 317 (2009).
[169] C. Van Cromphaut, V. G. De Resende, E. De Grave, and R. E. Vandenberghe, Meteorit. Planet. Sci. 42, 2119 (2007).
[170] I. Casanova, T. Graf, and K. Marti, Science 268, 540 (1995).
[171] A. N. Krot, N. I. Zaslavskay, M. I. Petaev, N. N. Kononkova, G. M. Kolesov, and L. D. Barsukova, Meteoritics 27, 465 (1992).
[172] B. Mason, Am. Sci. 55 (4), 429 (1967).
[173] K. Bugayev, Y. Bychkov, Y. Konovalov, V. Kovalenko, E. Tretyakov, "Iron and Steel Production" (MIR, Moscow, 1971). ISBN: 0-89499-109-4.
[174] J. D. van der Waals, Over de Continuiteit van den Gasen Vloeistoftoestand (On the continuity of the gas and liquid state). Ph.D. thesis, Leiden, Netherlands (1873); The equation of state for gases and liquids, Nobel Lectures in Physics 1901-1921, p. 254–265 (1910).
[175] V. D. Blank, Y. Y. Boguslavsky, M. I. Eremets, E. S. Itskevich, Y. S. Konyaev, A. M. Shirokov, and E. I. Estrin, Zh. Eksp. Teor. Fiz. 87, 922 (1984).
[176] S. Sasaki, R. Ishiguro, F. Caupin, H. J. Maris, S. Balibar, Science 313, 1098–1100 (2006).
[177] K.O. Keshishev, A. Ya. Parshin, A.V. Babkin, JETP Lett. 30, 5659 (1979).
[178] P. Kapitza, Nature 141, 74 (1938).
[179] A. B. Belonoshko and R. Ahuja, Phys. Earth Planet. In. 102, 171 (1997).
[180] A. B. Belonoshko, S. Arapan, and A. Rosengren, J. Phys.: Condens. Matter 23, 485402 (2011).
[181] L. Koci, A. B. Belonoshko, and R. Ahuja, Phys. Rev. B 73, 224113 (2006).

[182] A. B. Belonoshko, P. I. Dorogokupets, B. Johansson, S. K. Saxena, and L. Koci, Phys. Rev. B 78, 104107 (2008).
[183] A. B. Belonoshko, Condens. Matter Phys. 13 (2), 23605 (2010).
[184] D. Sheppard, P. H. Xiao, W. Chemelewski, D. D. Johnson, and G. Henkelman, J. Chem. Phys. 136, 074103 (2012).
[185] N. A. Zarkevich and D. D. Johnson, J. Chem. Phys. 142, 024106 (2015).
[186] B. Dupe, B. Amadon, Y. P. Pellegrini, and C. Denoual, Phys. Rev. B 87, 024103 (2013).
[187] G. Kresse and J. Hafner, Phys. Rev. B 49, 14251 (1994).
[188] G. Kresse and J. Furthmüller, Phys. Rev. B 54, 11169 (1996).
[189] G. Kresse and J. Furthmüller, Comp Mater Sci 6, 15 (1996).
[190] J. P. Perdew, J. A. Chevary, S. H. Vosko, K. A. Jackson, M. R. Pederson, D. J. Singh, and C. Fiolhais, Phys. Rev. B 46, 6671 (1992).
[191] J. P. Perdew, Phys Lett A 165, 79 (1992).
[192] P. E. Blöchl, Phys. Rev. B 50, 17953 (1994).
[193] G. Kresse and D. Joubert, Phys. Rev. B 59, 1758 (1999).
[194] D. D. Johnson, Phys. Rev. B 38, 12807 (1988).
[195] H. J. Monkhorst and J. D. Pack, Phys. Rev. B 13, 5188 (1976).
[196] V. N. Zharkov and V. A. Kalinin, Equations of state for solids at high pressures and temperatures (Consultants Bureau, New York, 1971).
[197] F. D. Murnaghan, Proc. Natl. Acad. Sci. USA 30, 244 (1944).
[198] F. Birch, Phys. Rev. 71, 809 (1947).
[199] H. L. Zhang, S. Lu, M. P. J. Punkkinen, Q. M. Hu, B. Johansson, and L. Vitos, Phys. Rev. B 82, 132409 (2010).
[200] X. Sha and R. E. Cohen, Phys. Rev. B 73, 104303 (2006).
[201] A. P. Jephcoat, H. K. Mao, and P. M. Bell, J. Geophys. Res. Solid Earth 91, 4677 (1986).
[202] N.V. Kadobnova and A.M. Bratkovskii, Mechanical Properties of Materials (Chapter 3), in Fizicheskie Velichiny (ed. I.S. Grigoryev, E.Z. Meylikhov), Moscow, EnergoAtomIzdat (1991). ISBN 5-283-04013-5.
[203] S. Klotz and M. Braden, Phys. Rev. Lett. 85, 3209 (2000).
[204] X. W. Sha and R. E. Cohen, Phys. Rev. B 81, 094105 (2010).
[205] G. Steinle-Neumann, L. Stixrude, and R. E. Cohen, Phys. Rev. B 60, 791 (1999).
[206] P. Haas, F. Tran, and P. Blaha, Phys. Rev. B 79, 085104 (2009).
[207] L. Stixrude, R. E. Cohen, and D. J. Singh, Phys. Rev. B 50, 6442 (1994).
[208] A. Dewaele, P. Loubeyre, F. Occelli, M. Mezouar, P. I. Dorogokupets, and M. Torrent, Phys. Rev. Lett. 97, 215504 (2006).
[209] V. E. Fortov, V. V. Yakushev, K. L. Kagan, I. V. Lomonosov, V. I. Postnov, T. I. Yakusheva, JETP Lett. 70 (9), 628–632 (1999). Translated from: Pisma Zh. ksp. Teor. Fiz. 70 (9), 620–624 (1999).
[210] M. Hanfland, K. Syassen, N. E. Christensen, and D. L. Novikov, Nature 408, 174-178 (2000).
[211] T. Matsuoka and K. Shimizu, Nature 458, 186 (2009).
[212] A. F. Goncharov, V. V. Struzhkin, H. K. Mao, and R. J. Hemley, Phys. Rev. B 71, 184114 (2005).
[213] C. L. Guillaume, E. Gregoryanz, O. Degtyareva *et al.*, Nature Physics 7, 211214 (2011).